Journal of Photochemistry & Photobiology, B: Biology 235 (2022) 112567

Contents lists available at ScienceDirect

Journal of Photochemistry & Photobiology, B: Biology

journal homepage: www.elsevier.com/locate/jphotobiol

Responses of melanoma cells to photobiomodulation depend on cell pigmentation and light parameters

Carolina Gouvêa de Souza Contatori [a], Camila Ramos Silva [a], Saulo de Toledo Pereira [a], Maria Fernanda Setúbal Destro Rodrigues [b], Arthur Cássio de Lima Luna [c], Marcia Martins Marques [d,e], Martha Simões Ribeiro [a,*]

[a] Center for Lasers and Applications, Nuclear and Energy Research Institute (IPEN/CNEN), São Paulo, SP, Brazil
[b] Postgraduate Program in Biophotonics Applied to Health Sciences, Nove de Julho University (UNINOVE), São Paulo, SP, Brazil
[c] Medicine Faculty, Health Department III, Nove de Julho University (UNINOVE), Osasco, SP, Brazil
[d] AALZ – Aachen Dental Laser Center, RWTH Aachen University, Aachen, Germany
[e] School of Dentistry, Ibirapuera University, São Paulo, SP, Brazil

ARTICLE INFO

Keywords:
Amelanotic melanoma
Low-level laser therapy
Near-infrared laser
Neoplasm invasion
Preclinical
Red laser
VEGF

ABSTRACT

Melanoma is a highly aggressive skin cancer that requires new approaches for its management. Low-level laser therapy, currently named photobiomodulation therapy (PBM), has been used to improve different conditions but its effects and safe use on melanoma remain unexplored. Herein, we investigated the PBM impact on melanoma cells differing by pigmentation using near-infrared (NIR) and red lasers *in vitro*. *In vivo*, we evaluated the effects of the red laser on melanoma-bearing mice. Amelanotic (SK-MEL-37) and melanotic (B16F10) cells were exposed *in vitro* to a NIR (780 nm, 40 mW) or a red laser (660 nm, 40 mW) in 3 different light doses: 30, 90, and 150 J/cm^2 and responses were assessed regarding mitochondrial activity, invasiveness, migration, and VEGF production. *In vivo*, melanoma-bearing mice received the red laser delivering 150 J/cm^2 directly to the tumor on 3 consecutive days. Mice were monitored for 15 days regarding tumor progression and mouse survival. We noticed that amelanotic cells were unresponsive to NIR light. In contrast, NIR irradiation at 30 J/cm^2 promoted an increase in the invasiveness of pigmented cells, even though all light doses have inhibited cell migration. Regarding the red laser on pigmented cells, the highest light dose (150 J/cm^2) decreased the VEGF production and migration. *In vivo,* melanoma-bearing mice treated with red laser showed smaller tumor volume and longer survival than controls. We conclude that PBM appears to be safe for amelanotic non-pigmented melanoma but triggers different responses in melanotic pigmented cells depending on light parameters. Additionally, a high dose of red laser impairs the invasive behavior of melanoma cells, probably due to the decrease in VEGF synthesis, which may have contributed to tumor arrest and increased mouse survival. These findings suggest that red laser therapy could be a new ally in the supportive care of melanoma patients.

1. Introduction

Skin cancer is the most common cancer worldwide and can be melanoma or nonmelanoma [1]. Melanoma is a malignant lesion affecting melanocytes, *i.e.,* melanin-producing cells, whose function consists in the coloring and defense of the skin against ultraviolet (UV) radiation [2]. Its incidence is estimated at 133.000 new cases each year according to the World Health Organization (WHO) [3].

The main environmental risk factor for this neoplasm development is exposure to UV radiation. However, the origin of this disease is also related to genetic factors, such as genetic susceptibility from the host and family history [4,5]. The neoplasm is characterized by a lesion of irregular edges presenting asymmetric variation, colour diversity, and diameter increase. This type of cancer is highly curable if detected at early stages [5,6]. On the other hand, this condition represents the most aggressive and deadliest form of skin cancer, which is associated with its great metastatic potential [2].

Frequently, malignant melanoma can be misdiagnosed due to its

* Corresponding author at: Centro de Lasers e Aplicações, Instituto de Pesquisas Energéticas e Nucleares (IPEN/CNEN), Av. Prof. Lineu Prestes, 2242, 05508-000, Brazil.
E-mail address: marthasr@usp.br (M.S. Ribeiro).

https://doi.org/10.1016/j.jphotobiol.2022.112567
Received 10 March 2022; Received in revised form 29 August 2022; Accepted 8 September 2022
Available online 13 September 2022

different clinical presentation and similarity to various benign-looking melanocytic and non-melanocytic lesions [7]. Additionally, amelanotic melanomas are a rare subtype of melanoma that present a harder diagnostic challenge. They have a higher mitotic rate, frequent ulceration, higher tumor stage, and lower survival than pigmented melanomas, often being confounded for benign spots, scars, or cysts [8].

The features of the tumor, such as location, stage, and genetic profile, in addition to the patient's general health and age, are related to the melanoma treatment options, which could be surgery, chemotherapy, targeted therapy, and, more recently, immunotherapy. These therapies can be administered as single agents or in combination [9]. Surgery is the most common treatment for this condition and, even for melanomas at early stages, this procedure is invasive leaving hideous scars. Consequently, the surgery can cause social disorders and directly influence the patient's quality of life and recovery from treatment [6,9].

Light-based technologies to fight cancer have promoted great interest worldwide due to the search for less invasive forms of treatment. Photodynamic therapy (PDT) is the most common and has been used since the 80's to treat different types of solid cancers [10]. Low-level laser therapy, also termed photobiomodulation therapy (PBM), on the other hand, uses only light (usually red or near-infrared (NIR) from lasers or LEDs) to produce physiological functions with no heating to cells and tissues [11]. PBM has been used to promote ulcer healing [12], recover spinal cord injury [13], alleviate acute pain [14], *etc.* PBM is also applied to mitigate adverse side effects resulting from conventional cancer therapies such as oral mucositis, radiodermatitis, and lymphedema [15]. However, PBM's effects on cancer are unclear as it appears to exert stimulatory, inhibitory, or even no influence [16,17]. Light parameters such as wavelength and radiant exposure (or light dose) are key factors to trigger target cell signaling pathways and outcomes [18]. Besides, the cell type could also play a role in the photobiological response.

Due to the use of PBM as support of care in cancer patients and the possibility of PBM practitioners unintentionally irradiating undiagnosed amelanotic melanoma, which is non-pigmented and can resemble other skin cancers, we have been motivated in investigating the impact and safety of PBM using a near-infrared (NIR) and a red laser on B16F10 and SK-MEL-37 lineages, which exhibit the presence and absence of pigmentation, respectively [19]. We focused our attention on the ability of PBM to influence cell metabolic activity (MA) depending on nutritional growth conditions, vascular endothelial growth factor (VEGF) production, invasiveness, and migration. We also verified the cell response to different light doses. As a result, we conducted an *in vivo* study applying the red laser directly to the tumor originating from a melanin-producing cell line (murine) on melanoma-bearing C57BL/6 mice.

2. Materials and Methods

2.1. Cell Culture

The SK-MEL-37 amelanotic cutaneous melanoma cell line originated from a malignant melanoma of a rectal tumor. The B16F10 cell line was established from a primary cutaneous mouse C57BL/6 melanoma that produces melanin. B16F10 and SK-MEL-37 cells were cultured in RPMI 1640 medium (Vitrocell, Brazil) supplemented with fetal bovine serum (FBS), 100 U/mL penicillin (Sigma, USA), and 100 μg/mL streptomycin (Sigma, USA). The cells were maintained at 37 °C in a humid atmosphere containing 95% air and 5% carbon dioxide (CO_2). The culture medium was changed once every 2 days. After the cells reached 70% confluence they were trypsinized using 0.25% trypsin (Sigma, USA) and then centrifuged at 300 *g* for 300 s and plated for the assays. The cell cultures were submitted to cell metabolism, VEGF synthesis, invasiveness, and migration assays.

2.2. Photobiomodulation Protocol

The PBM was performed with a laser (Twin Flex Evolution, MMOptics Ltda, Brazil) emitting at $\lambda = 780$ nm and/or 660 nm with an output power of 40 mW, and irradiance of approximately 1 W/cm^2. The irradiation was performed 24 h after the cell seeding into a 96-well plate. A volume of 200 μL corresponding to a height of 0.8 cm was submitted to light doses of 30 (G30), 90 (G90), and 150 (G150) J/cm^2. Control cells (G0) were not irradiated. The cells were irradiated uniformly upwards so that the laser tip (0.04 cm^2) was placed in direct contact with the middle of the bottom of the plaque to irradiate a single well. The plates were covered with a black card and the wells around the irradiated one were left empty to prevent light scattering during laser irradiation. Temperature changes were monitored by positioning a thermometer in the well when the highest light doses were used.

For the invasion assay, the irradiation was done directly in the pellet formed at the bottom of the centrifugation tube, on the same day of the cell seeding. The conic tube was also covered with a black card. For the migration assay, we used 6-well plates. In this case, the laser tip uniformly scanned the well. The PBM parameters are summarized in Table 1.

2.3. Metabolic Activity (MA)

Melanoma cells of both cell lines were seeded at the final concentration of 5×10^3 cells per well in ideal nutritional condition (10% FBS) or deficit nutritional condition (5% FBS). Twenty-four-h after laser irradiation, 20 μL of MTT (3-(4,5-dimethylthiazol-2-yl)-2,5-diphenyltetrazolium-bromide) (Sigma, USA) were added at the concentration of 5 mg/mL [20]. The cells were incubated in an atmosphere comprising 5% CO2 at 37 °C for 3 h. The formazan crystals (colorimetric product) were solubilized with 100 μL of dimethyl sulfoxide (DMSO). The optical density was read in a microplate reader (Spectramax M4, Molecular Devices, USA) at $\lambda = 570$ nm following 30 min from the solubilization of the crystals.

2.4. VEGF Measurement

Melanoma cells of both cell lines were cultured under starvation (5% FBS) and seeded in 96-well plates at a density of 5×10^3 cells per well, in triplicate. These cells were submitted to irradiation twenty-four-h later. Then, 24 h after irradiation the culture supernatants were collected and stored at −20 °C for later VEGF measurement.

VEGF synthesis was assessed by using specific ELISA kits (Sigma, USA) following the manufacturer's instructions. The absorbance was read in a microplate reader (SpectraMax, Molecular Devices, USA) using a 450 nm filter.

2.5. Transwell Cell Invasion Assay

Transwell cell invasion assay was carried out with a Transwell system (Corning, USA) composed of an insert (upper chamber) placed in the culture wells (lower chamber) of 24-well plates divided by an 8 μm pore size filter. One hundred-μL of Matrigel (Corning, USA) was diluted in FBS-free RPMI following the manufacturer's instructions and applied on the top of the filter in the upper chamber. Six-hundred-μL of RPMI

Table 1
Parameters used for irradiation of pigmented (B16F10) and amelanotic (SK-MEL-37) melanoma cells.

Group	Exposure time (s)	Energy (J)	Radiant exposure (J/cm^2)
G0	0	0	0
G30	30	1.2	30
G90	90	3.6	90
G150	150	6	150

with 10% FBS was added to the bottom well.

Following the irradiation of the cells in the pellets at the bottom of the Eppendorf tubes, irradiated and non-irradiated cells were resuspended in a serum-free medium and 1×10^5 cells/well were added to the upper compartment of the Transwell chamber. Culture plates were incubated in an atmosphere comprising 5% CO2 at 37 °C for 24 h. Then, non-migrated cells were removed from the upper compartment while migrated cells were fixed in 4% paraformaldehyde and methanol and stained with violet crystal. Migrated cells represented by streaked purple cells were counted in an inverted microscope (AE31, Motic, Canada) directly on the plate with the aid of a cell counter.

2.6. Migration Assay

The pigmented cell line (treated and non-treated) was seeded in a 6-well plate at a density of 2×10^5 cells/well in triplicate at two different moments. At the time cells reached confluence, a scratch was performed to disrupt the confluent cell monolayer with a 10 μL pipette tip in the shape of a single line. Then, the medium was aspirated and each well was washed with phosphate-buffered saline (PBS) following the addition of fresh medium. Immediately after the injury, B16F10 cells were submitted to PBM (see Table 1) by scanning the well. Cells were photographed immediately and at 3, 12, 24, and 36 h after the scratch. The scratch area was measured using ImageJ software. The percentage of cell migration was calculated using the following equation:

$$\frac{\text{Scratch area}_{(0h)} - \text{Scratch area}_{(nh)}}{\text{Scratch area}_{(0h)}} \text{ x } 100, \text{ where } n = 3,\ 12,\ 24 \text{ and } 36$$

2.7. Absorption Coefficient Calculation

B16F10 and SK-MEL-37 cells were trypsinized and a density of 10^6 cells/mL was centrifuged at 300 *g* for 5 min at room temperature in a conical tube. Then, the medium was aspirated and the pellet was washed with 10 mL of ice-cold PBS. Cells were again centrifuged at 300 *g* for 5 min to decant PBS and excess supernatant aspirated. Following this step, 100 μL of RIPA lysis buffer were added and the lysate was incubated for 15 min on ice. The lysate was sonicated three times for 2 s each with 1 min rest on ice between every two-second pulse and then incubated on ice for 15 min. The lysate was centrifuged at 13.000 *g* for 5 min at 4 °C and the supernatant was collected into new microtubes. Then, we added 100 μL of the supernatant and 100 μL of PBS in a quartz cuvette (L = 1 cm), and the absorbance (A) was read in a spectrophotometer (Cary 5000 UV-VIS-NIR, Agilent) from 400 to 800 nm.

The absorption coefficient (α) was calculated from absorbance, which is defined as log (I_0/I), where I_0 is the light intensity before the sample and I is the intensity of the beam passed through the sample. From Beer's law, α = A/L·log (e) = 2.302·A, where L is the optical path length (1 cm).

2.8. In vivo Assay

All experiments were approved by the Ethics Committee on Animal Use of the Nuclear and Energy Research Institute (IPEN). Male C57BL/6 mice ($n = 8$) with 8 weeks of age and body mass of approximately 20 g were subcutaneously inoculated with 1×10^6 B16F10 cells on the right flank.

The animals were monitored daily until it was possible to observe a delimited nodule in all animals (approximately 7 days). At that moment, we initiate the measurement of the tumor volume with a digital caliper according to the equation:

$$V = 0.5 \times C \times L^2$$

where V is the volume in cm^3, C is the length and L is the width of the tumor, both in cm.

After 15 days, when the tumor volume reached approximately 1.0 cm^3, the animals were randomly divided into control and PBM groups ($n = 4$/group). For the PBM group, the red laser tip was placed in contact with the middle of the tumor for 150 s (150 J/cm^2/day) for three consecutive days [21]. Mice were monitored for 15 days. Control animals were equally manipulated but not irradiated for spontaneous tumor development. Mice of both groups were then euthanized on day 16 due to the humane endpoint.

2.9. Statistical Analysis

Numerical values are presented as means ± standard error of the mean (SEM). Results were analyzed by one-way analysis of variance (ANOVA) and Fisher's test to identify differences among groups using Graph Pad Prism 7.0 software. *In vitro* assays were conducted at least twice, in triplicate. *In vivo*, we used the Student's *t*-test for group comparison and the Log-Hank test for the survival analysis. Statistically significant differences were admitted when $p < 0.05$.

3. Results

3.1. The Near-Infrared Laser Does Not Influence the Metabolic Activity of Melanoma Cell Lines

No statistically significant differences were noticed among groups. The irradiated groups presented similar metabolic activity in comparison to G0 regardless of growth condition (Fig. 1a). SK-MEL-37 cells showed a reduction of approximately 10% between groups G0 and G30 (0.49 ± 0.05 *versus* 0.43 ± 0.05, respectively) for cells cultured in ideal nutritional conditions. On the other hand, under deficit conditions, an increase of around 28% was observed for the same groups (0.31 ± 0.03 *versus* 0.4 ± 0.03, respectively).

Fig. 1b presents the mitochondrial activity for B16F10 cells (producing a melanin cell line). No statistically significant differences were observed among groups regardless of the growth condition. Under the ideal growth condition, G30 (0.54 ± 0.05) and G90 (0.56 ± 0.05) groups demonstrated an increase of approximately 15% when compared to the control group (0.49 ± 0.04), while G150 (0.49 ± 0.05) presented a similar metabolic activity to G0. In contrast, we observed an opposite behavior under stress, since G30 (0.26 ± 0.03) demonstrated a reduction of 10%, while G90 (0.33 ± 0.03) and G150 (0.33 ± 0.04) presented an increase of approximately 12% in comparison to G0 (0.3 ± 0.03).

3.2. The Near-Infrared Laser Does Not Influence the Production of VEGF by Melanoma Cell Lines

Fig. 2 illustrates graphically the response of human (SK-MEL-37 cell line) and murine (B16F10 cells) melanoma cells regarding the VEGF production. No statistically significant differences in VEGF concentration were noticed for both cell lines regardless of the light dose used. The human cell line demonstrated a similar behavior between G30 (135 ± 13 pg/mL) and G150 (127 ± 11 pg/mL) in comparison to G0 (130 ± 8 pg/mL), while G90 (122 ± 11 pg/mL) presented a decrease about 6.5%. On the other hand, murine melanoma cells, those that are melanin-producing, showed an increase of 32% in G90 (33 ± 8 pg/mL). Moreover, G30 (19 ± 5 pg/mL) and G150 (23 ± 5 pg/mL) presented reduction when compared to control group (25 ± 4 pg/mL).

3.3. The Near-Infrared Laser Promotes Cell Invasion but Inhibits Migration of Pigmented Cells Depending on the Light Dose

Fig. 3a exhibits the average number of cells that invaded the Matrigel for SK-MEL-37 and B16F10 cells. No statistically significant differences were observed between treated and control groups regarding the human melanoma cells (SK-MEL-37). There was a reduction of about 16% in G30 (17 ± 1) while G150 (20 ± 3) presented a decrease of 5% compared

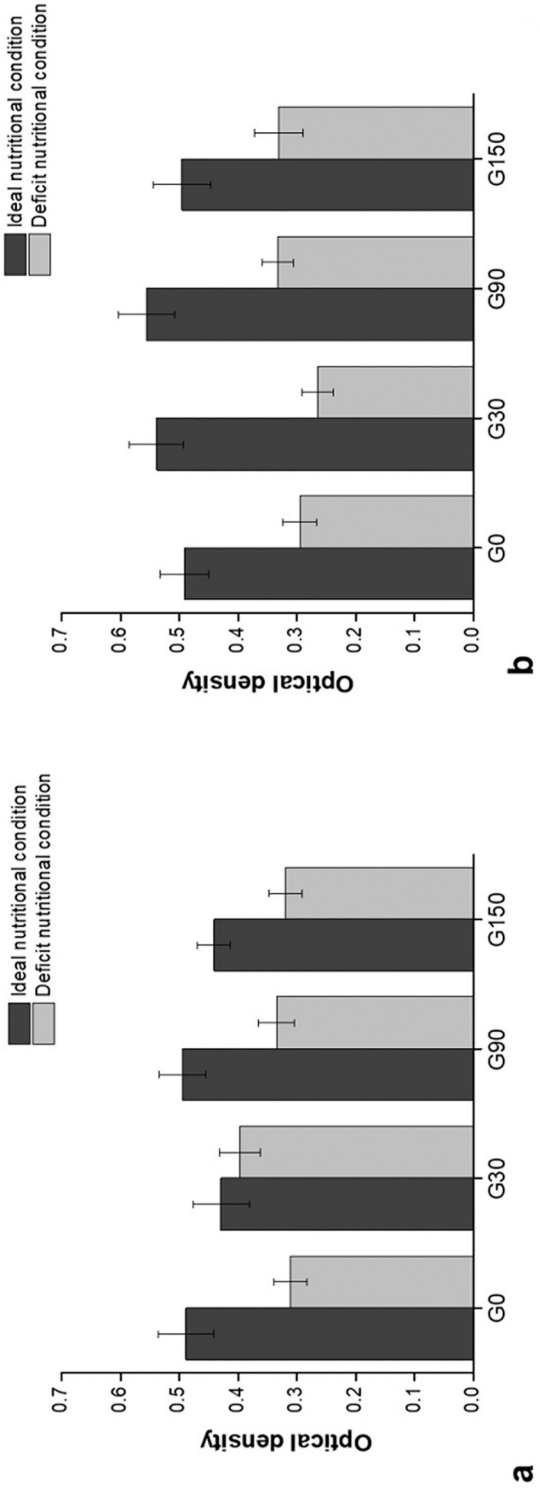

Fig. 1. Graphic representation of the optical density (metabolic activity) for cells cultured under ideal and deficient nutritional conditions for amelanotic (SK-MEL-37) (a) and pigmented melanoma cells (B16F10) (b). The data are presented as means ± SEM values.

to G0 (21 ± 2).

In contrast, we observed significantly higher invasiveness regarding the melanin-producing murine cells (B16F10) in the same conditions. The lowest radiant exposure, G30, presented an increase of about 33% (35 ± 2) in comparison to the control group (G0, 27 ± 3). Nonetheless, G90 (29 ± 2) and G150 (23 ± 1) did not significantly influence the cell invasion behavior of B16F10 cells when compared to G0.

Fig. 3b (G0) and 3c (G30) exhibit representative images of B16F10 cells that invaded the Matrigel, depicted by purple blots.

Considering the effects observed in both cell lines and that only pigmented melanoma cells when irradiated with the laser emitting at λ = 780 nm demonstrated a higher invasive potential, we asked whether NIR could also stimulate cell migration. We observed that 3 and 12 h post-irradiation, G90 showed a significantly higher percentage of cell migration than G0 (p = 0.04 and 0.01, respectively). Surprisingly, all NIR light doses inhibited cell migration after 36 h (Fig. 4).

Driven by curiosity, we also inquired whether varying the wavelength would modify the response of these cells. Therefore, the B16F10 cell line was exposed to a red laser at λ = 660 nm. Experimental groups were the same as displayed in Table 1.

3.4. The Red Laser Increases the Metabolic Activity of the Pigmented Cell Line Depending on the Light Dose

The metabolic activity in all treated groups of cells grown under ideal nutritional conditions was similar. Differently, for cells grown under deficit nutritional conditions, there was a significant increase of 26% (p = 0.01) in G90 in comparison to G0 (Fig. 5).

3.5. The Red Laser Significantly Reduces the VEGF Production and Slows Down Cell Migration Depending on the Light Dose

The VEGF concentration for B16F10 cells showed a statistical significant decrease of about 26% (p = 0.02) for G150 (35 ± 3 pg/mL) when compared to G0 (49 ± 4 pg/mL) 24-h after laser irradiation (Fig. 6a). The other groups (G30 and G90) presented similar VEGF production to G0 (control).

Additionally, groups G90 (12 ± 2) and G150 (11 ± 0.6) presented a lower number of invasive cells than G0 (19 ± 4) when submitted to the red laser. Indeed, the highest light dose (150 J/cm^2) promoted a decrease of approximately 60% in cell invasiveness, even though no statistically significant differences were observed (Fig. 6b). However, the highest dose was able to significantly inhibit cell migration 24 (p = 0.000013) and 36 h (p = 0.02) post-irradiation (Fig. 7).

For a deeper understanding of the role of light absorbed by pigmented and non-pigmented cells, we measured the cell absorption coefficient (Fig. 8). The absorption coefficient determines how far light in a material of a given wavelength can penetrate before being absorbed. Overall, B16F10 shows slightly higher α than SK-MEL-37 cells, even though spectra were quite similar. Absorption bands around 400, 600, and 750 nm can be observed.

Regardless of the melanoma cell, α ≅ 0.11 cm^{-1} for 660 and 780 nm. This means that light could penetrate approximately 9 cm before being completely absorbed. Yet, it is worth mentioning that the temperature variation was around 1 °C regardless of the melanoma cell and wavelength.

Considering the surprising results obtained with the red laser on pigmented cells, and envisaging the clinical use of PBM as a possible ally to the supportive care for melanoma patients, we designed a preliminary study to assess the effects of the light dose of 150 J/cm^2 applied directly to the tumor *in vivo*.

3.6. The Red Laser Inhibits the Tumor Growth and Extends the animal's Survival

We noticed that the tumor volume for control and PBM groups

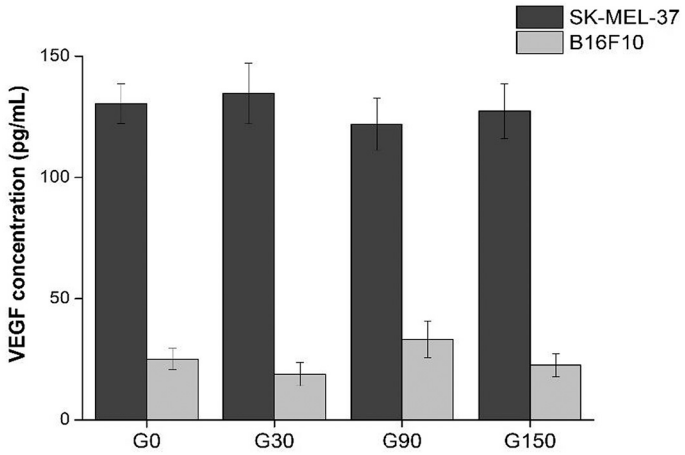

Fig. 2. Graphic representation of the VEGF concentration for amelanotic (SK-MEL-37) and pigmented (B16F10) melanoma cells 24 h after irradiation using an infrared laser (λ = 780 nm) and different light doses. The data are presented as means ± SEM values.

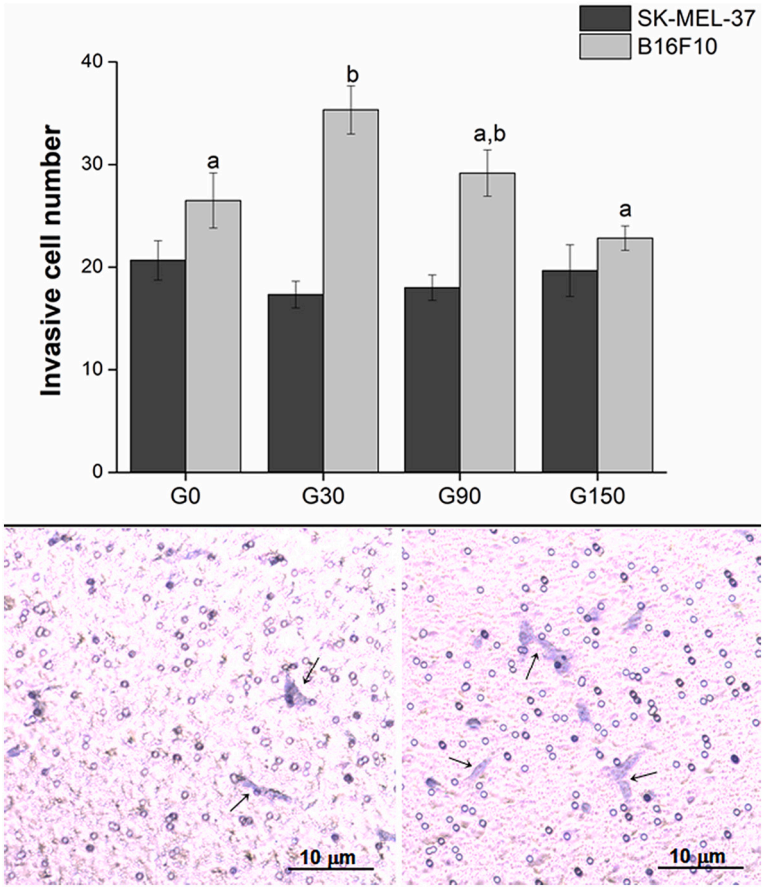

Fig. 3. Graphic representation of the number of amelanotic (SK-MEL-37) and pigmented (B16F10) cells that invaded the matrigel in search of nutrients. Data are presented as means ± SEM values. Different lowercase letters represent statistically significant differences between groups of the same cell line (a); Representative photomicrographs of migrated cells (arrows) for control (b) and G30 (c) groups. (For interpretation of the references to colour in this figure legend, the reader is referred to the web version of this article.)

presented a sigmoidal pattern, *i.e.*, the progression goes through exponential, linear, and asymptotic phases (Fig. 9a). However, the PBM group showed lower growth than untreated mice, mainly from the 5th day. At this time point, the difference between the treated and control group was around 43% (4 ± 2 cm^3*versus* 7 ± 1 cm^3). After the 7th day, we detected statistically significant differences between groups ($p = 0$). Indeed, on the 15th day, the tumor volume was around 50% smaller for the PBM group. Fig. 9b illustrates the tumor volume for control and PBM groups at the end of the experimental period.

We also observed that animals of the control group showed 50% of survival on the 10th day (Fig. 9c). On the 16th, this value was 25% (only 1 animal survived). In contrast, the irradiated group exhibited 100% survival, and a statistically significant difference ($p = 0.007$) was detected when compared with the control group.

4. Discussion

A recent systematic review about the effects of low-level laser therapy on tumor cells *in vitro* concluded that there is a wide discrepancy in laser parameters such as wavelength, light doses, and type of laser that

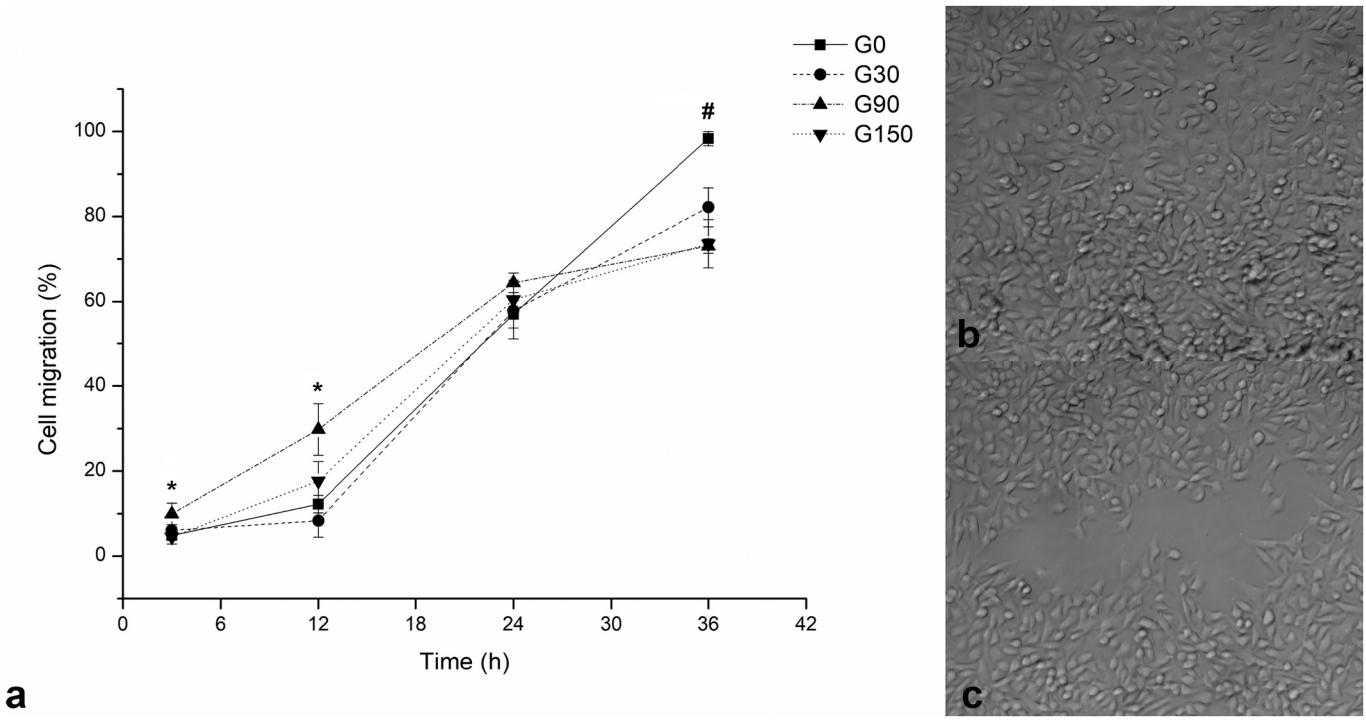

Fig. 4. Graphic representation of the percentage of cell migration of pigmented (B16F10) cells irradiated with a NIR laser (λ = 780 nm) in different radiant exposures (a). The data are presented as means ± SEM values. * represents moments in which cell migration for G90 is significantly faster than control (G0). # represents the moment in which cell migration is significantly inhibited for all irradiated groups. Representative images of scratch closure for G0 (b) and G90 (c) at 36 h post-irradiation.

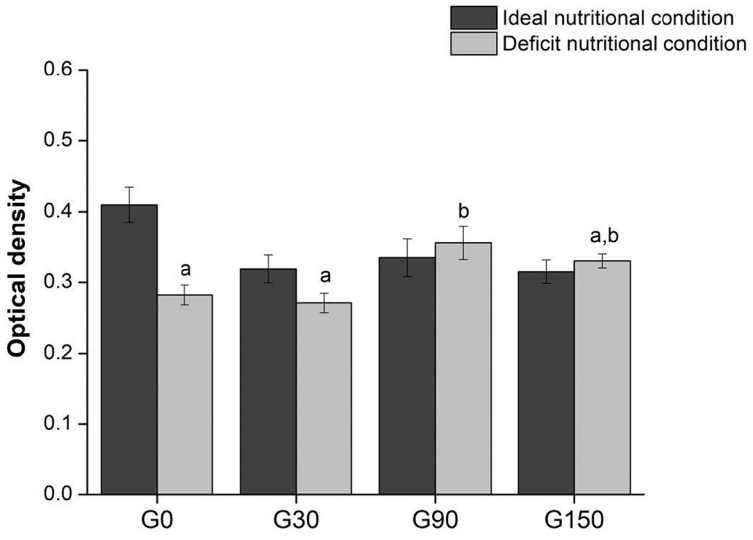

Fig. 5. Graphic representation of the optical density (metabolic activity) for pigmented (B16F10) melanoma cells cultured in ideal nutritional conditions and nutritional deficit conditions. The data are presented as means ± SEM values. Different lowercase letters represent statistically significant differences among groups of cells grown under the same nutritional condition.

averts a standardization of irradiation protocol [22]. Indeed, some included studies showed an increase while other studies showed a decrease in tumor cell proliferation. The authors highlighted the need for further studies to provide more solid evidence before using PBM in cancer patients, which motivated our work.

In our study, we used NIR and red lasers on melanoma cells to assess the cell response regarding metabolic activity, angiogenesis, cell invasion, and cell migration. We also measured temperature changes during irradiation under the highest light doses for both wavelengths and melanoma cells. As expected, no significant variation was noticed in temperature. Indeed, it is fairly well known that the amount of heat generated by optical illumination is critically dependent upon laser irradiance. Here, we used an irradiance of 1 W/cm^2, which is not expected to promote heat [23]. Besides, the absorption coefficient was approximately 0.11 cm^{-1} regardless of the wavelength and melanoma cell. Although we have used human amelanotic and murine melanotic cells, Oikawa and Nakayasu used melanin from melanotic and amelanotic clonal cell lines of mouse melanoma B16 and measured melanin absorbance, which decays exponentially from the ultraviolet to 580 nm [24]. Thus, substantial differences in absorbance are not expected for

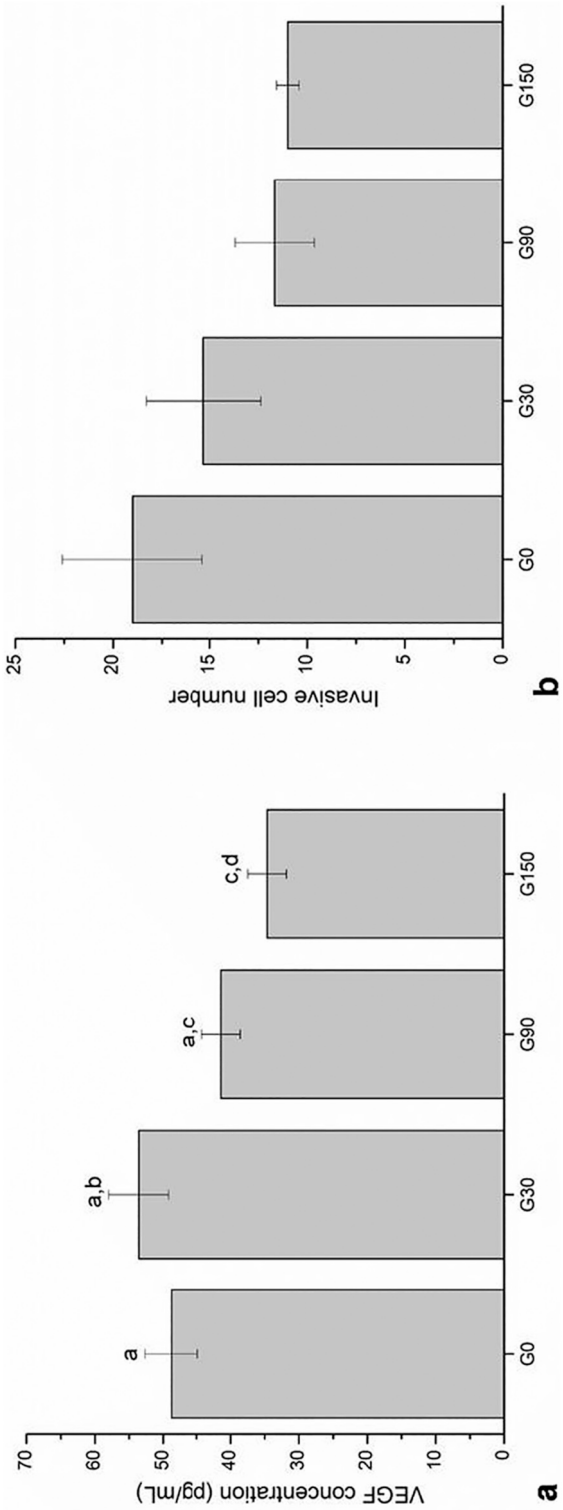

Fig. 6. Graphic representation of the VEGF concentration (a) and invasiveness (b) of pigmented (B16F10) cells irradiated with a red laser ($\lambda = 660$ nm) in different radiant exposures. The data are presented as means ± SEM values. Different lowercase letters represent statistically significant differences between groups.

longer wavelengths, regardless of the cell origin. These data are in agreement with our results.

We decided to apply the NIR laser because it is the most commonly reported to relieve pain [15,25] since infrared can penetrate deeper than red wavelengths into biological tissue [26]. We noticed that the pigmented melanoma cell line exposed to the lowest light dose (30 J/cm^2) presented a higher number of invasive cells than the unirradiated cells, even though all light doses inhibited cell migration 36 h after irradiation. In contrast, although the highest dose (150 J/cm^2) increased MA it was able to significantly inhibit cell migration and promote a significant reduction in VEGF synthesis by B16F10 cells under red light.

B16F10 and SK-MEL-37 melanoma cell lines exhibit similar growth, with a doubling time of 24.0 ± 4.0 and 28.6 ± 3.0 h, respectively [27]. Besides, it is known that tumors may develop tolerance to starvation due to an adaptation of metabolism to their microenvironment [28], and tumor cell cultures under deficit nutritional conditions seem to be sensitive to laser irradiation [29]. Thus, for the MA assay we cultured melanoma cells under normal and stress conditions.

No impact of NIR radiation was observed on the cell MA regardless of the light dose, cell line, or nutritional condition. Under red light, however, we noticed an increased metabolic activity depending on the light dose for cells in nutritional deprivation. This increase in the MA of pigmented cells exposed to the middle dose could be related to either hyperactive mitochondria or increased mitochondrial mass. Indeed, mitochondrial biogenesis and hyperactivation may lead to increased MA following ionizing radiation [30].

An increase in mitochondrial mass in irradiated cells could be obtained due to a blockage in the G2/M phase. Cells arrested in this phase would have a higher number of mitochondria, which may reduce more MTT to formazan and, consequently, promote an increase in MA [30]. Our data indicate that the middle dose promoted an increase in MA of pigmented cells by arresting them in the G2/M phase, which is consistent with the results reported by Silva et al. [31].

On the other hand, it is well known that melanoma cells are highly metastatic. For this reason, we were curious in assessing the PBM effects on cell VEGF production and invasiveness. To quantify VEGF, we cultured the cells under deficit nutritional conditions to activate pro-angiogenic molecules [32]. Our results showed that the NIR laser was not able to influence the VEGF production regardless of the cell line, and the light dose.

Differently, the irradiation of pigmented cells with the NIR laser showed that the lowest light dose promoted a significant increase in the number of invasive cells. Besides, NIR was able to hasten cell migration for the middle dose in the first 12 h following irradiation. The metastatic process involves the degradation of basement membranes and remodeling of the extracellular matrix by proteolytic enzymes, and B16F10 cells have elevated levels of proteases and glycosidases [33]. Our finding indicates that NIR may have promoted an increase in the activity of those degradative enzymes and, consequently, influenced the cell migration and invasiveness depending on the light dose. However, the NIR laser was not able to impact metabolic activity and angiogenesis as well as slowed down cell migration 36 h post-irradiation. These data suggest that migration and invasiveness promoted by NIR could be temporary. Malignant cells depend on oxygen and nutrients for their survival, therefore new vessel formation must coexist with the invasion process [32].

In contrast, we noted that the highest light dose significantly inhibited the VEGF synthesis and cell migration under red exposure. Besides, it decreased the number of invasive cells, even though no statistically significant differences were identified ($p = 0.05814$). These opposite results triggered by NIR and red lasers could be explained by light absorption by different chromophores in a different redox state [34]. Indeed, different chromophores may play distinct roles in driving different cell signaling pathways. The cytochrome *c* oxidase (CcO) is considered the prime photoacceptor of visible and NIR light and contains two redox-active copper sites (Cu_A and Cu_B) that are the absorbing

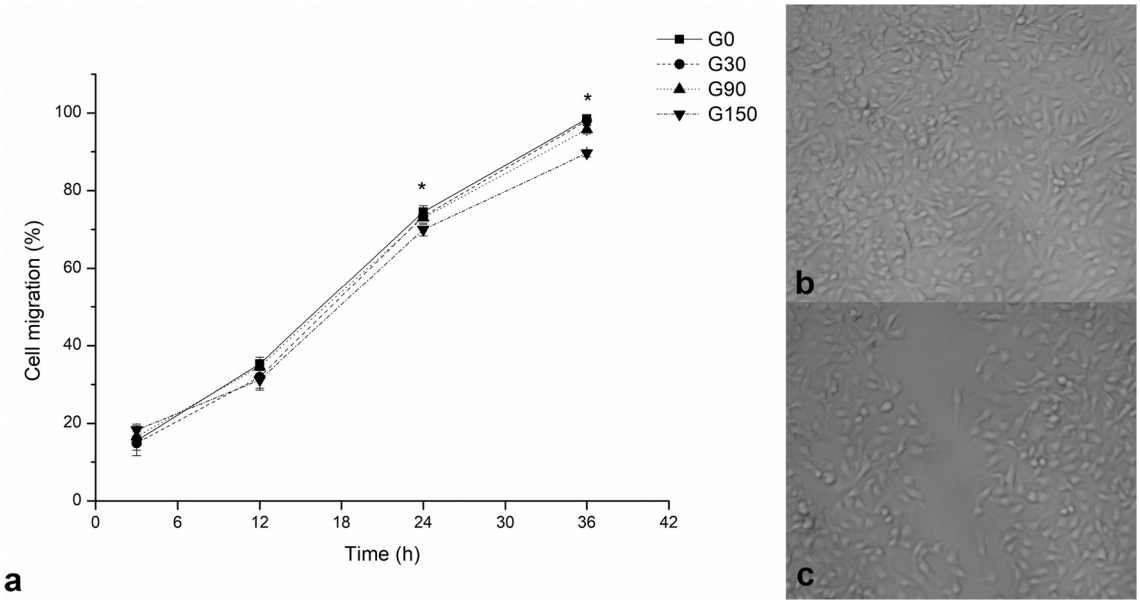

Fig. 7. Percentage of cell migration of pigmented (B16F10) cells irradiated with a red laser (λ = 660 nm) in different radiant exposures (a). The data are presented as means ± SEM values. * represents moments in which the percentage of cell migration for G150 was significantly lower than the control group (G0). Representative images of scratch closure for G0 (b) and G150 (c) at 36 h post-irradiation.

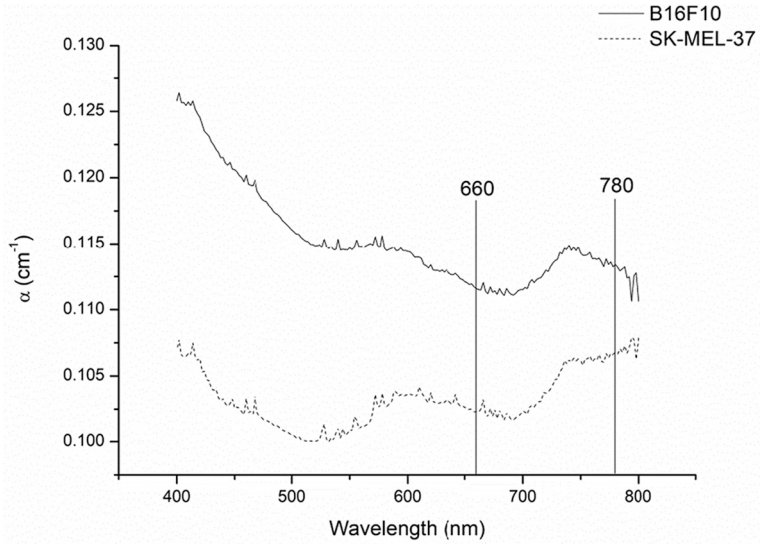

Fig. 8. Absorption coefficient of pigmented (B16F10) and non-pigmented (SK-MEL-37) melanoma cells. The wavelengths used in this work are highlighted.

chromophores [34]. Since metastatic melanoma cells have elevated levels of oxidative phosphorylation and mitochondrial respiration can be a key target for anti-melanoma therapies [35], it might be worth exploring the CcO photoactivity of pigmented melanoma cells following red and NIR irradiation.

Andreeva and colleagues showed that the dynamics of the response of two melanoma cell lines to NIR radiation (835 nm) were quite similar, even though some quantitative differences were noticed [36]. The authors reported stimulation of cell growth under low doses (around 0.17 J/cm^2) whereas a higher dose (2.76 J/cm^2) suppressed the cell growth rate. Based on their data, the authors hypothesized that mitochondria conditions in tumor cells may vary, resulting in different responses of melanoma cells to irradiation. Indeed, the mitochondria of melanotic melanoma differ considerably from those of amelanotic melanomas [37]. The amelanotic melanoma retains intact and active mitochondria whereas the melanotic presents low CcO activity. This may also explain why SK-MEL-37 cells were insensitive to light.

The unexpected findings with the red laser stimulated us to pursue an *in vivo* study foreseeing the use of PBM as an ally to anti-melanoma therapies. For this reason, we applied the light directly to the tumor. Interestingly, we observed that the red laser was able to arrest the tumor growth and extend mouse survival. Collectively, our data suggest that the red laser inhibited the growth by reducing VEGF production and, possibly, cell migration and invasiveness.

However, our results differ from those stated by Frigo et al. [21], even though we have used a red laser at 150 J/cm^2 applied for 3 consecutive days as reported by them. They showed no impact of the irradiation on tumor progression. We assume that the mouse strain is the principal difference between the studies. Frigo and colleagues used albino BALB/c mice, whereas we used black C57BL/6 mice, a more appropriate model to develop melanoma *in vivo*.

Ottaviani and collaborators also investigated the use of laser

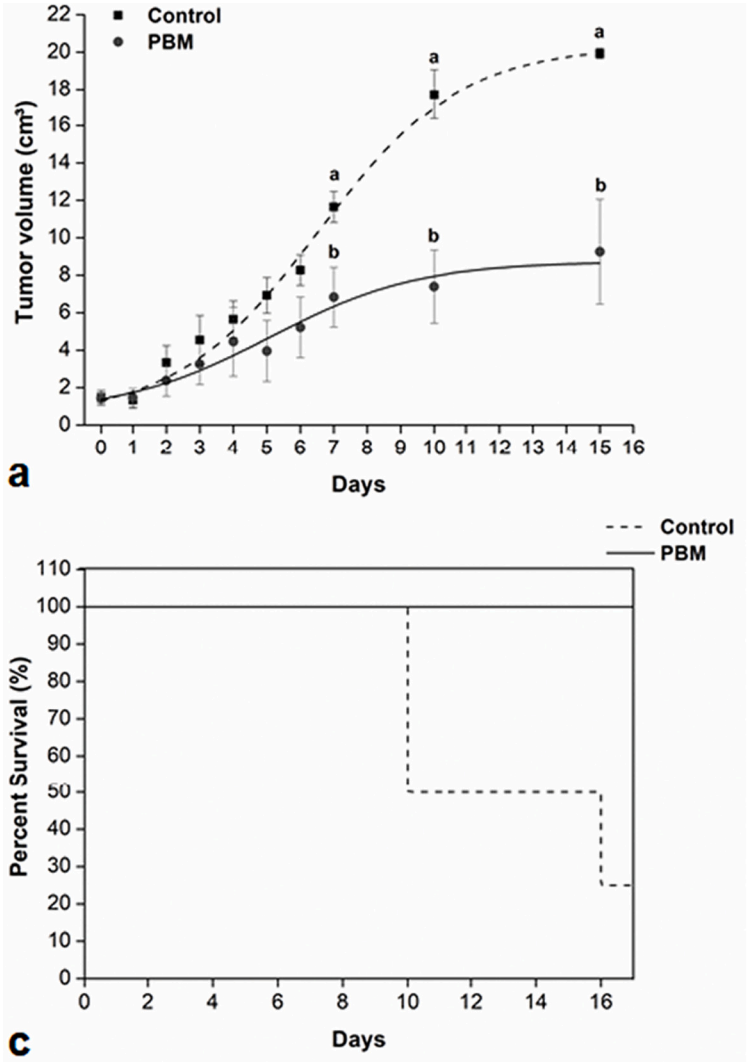

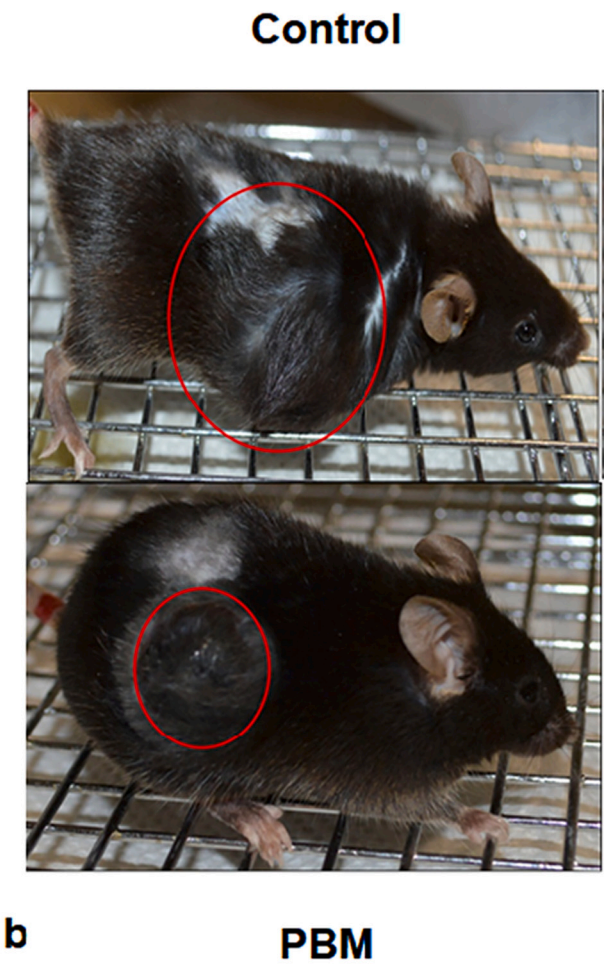

Fig. 9. PBM with a red laser (λ = 660 nm, *P* = 40 mW, D = 150 J/cm^2) in melanoma-bearing mice. Graphic representation of the tumor volume progression during the experimental period. PBM was applied on days 0, 1, and 2. Data are presented as mean ± SEM. Different lowercase letters represent statistically significant differences between groups (a); Representative images of melanoma-bearing mice for control and PBM groups before the euthanasia. The highlighted region refers to the tumor volume for each experimental group (b); Survival curves for control and PBM groups during the experimental period. Statistically significant differences were identified between groups (p = 0.007) (c).

irradiation on melanoma cells *in vitro* and *in vivo* [38]. Curiously, although red laser parameters were different from our study, they observed increased metabolic activity and reduced tumor progression in parallel with the recruitment of immune cells and vessel normalization *in vivo*. Our data confirm their findings and provide insights that enable us to hypothesize that the red laser arrested tumor progression by inhibiting cell migration and reducing VEGF synthesis. However, it is worth mentioning that the melanoma treatment depends on other parameters, as it is highly metastatic.

Interestingly, studies suggest that pigmented melanomas are more resistant to photo, radio, and chemotherapy [39,40]. Indeed, the process of melanin synthesis is highly controlled in normal melanocytes and therefore plays a protective role against chemical and physical aggression. However, melanin also appears to contribute to the malignant transformation of melanocytes and may be harmful in pathological conditions [39]. While the exact biological mechanisms related to melanogenesis after PBM remain unexplored, the exciting and unexpected results observed here using a red laser are very promising.

The main study limitation was the use of human amelanotic and murine melanotic cell lines, as murine melanomas do not reproduce some of the key characteristics of human melanoma [41]. However, Vincent and Postovit showed that even human melanoma cell lines and tumors differ at the transcriptional level due to the loss of immune components in cell culture [41]. Although *in vitro* studies carry other limitations, they are important to provide insights that allow future *in vivo* studies. Altogether, our results indicate that the responses of melanoma cells to photobiomodulation depend on cell pigmentation and light parameters. Further studies targeting other melanoma cell lines and melanogenesis are very welcome.

5. Conclusion

In summary, we have evaluated the effects of one single laser irradiation on two melanoma cell lines differentiated by pigmentation. No impact of NIR laser irradiation was noticed for amelanotic cells regardless of light parameters and PBM might be safe for undiagnosed amelanotic melanoma, which is non-pigmented and mimics other skin tumors from different origins. In contrast, our results demonstrated that PBM triggers opposite responses of pigmented cells depending on wavelength and light dose. NIR laser promoted invasiveness at a low dose and slowed down cell migration for all light doses, whereas the red laser at 150 J/cm^2 decreased cell invasiveness and significantly

inhibited cell migration and VEGF synthesis. In a suitable murine model, the red laser was able to arrest tumor growth and extend the mouse survival, even being applied directly to the tumor in more than one session. Together, our results encourage further studies to unravel the mechanisms behind PBM on pigmented melanoma. Additional studies encompassing melanoma current therapy combined with red light are also warranted.

Funding

This work was funded by Comissão Nacional de Energia Nuclear (CNEN) and the Instituto de Fotônica do Conselho Nacional de Desenvolvimento Científico e Tecnológico (INFO/CNPQ grant# 465763/2014-6). Carolina Gouvêa de Souza Contatori was supported by scholarship from Coordenação de Aperfeiçoamento de Pessoal de Nível Superior (CAPES).

CRediT authorship contribution statement

Carolina Gouvêa de Souza Contatori: Data curation, Formal analysis, Investigation, Methodology, Visualization, Writing – original draft. **Camila Ramos Silva:** Data curation, Formal analysis, Investigation, Methodology, Visualization, Writing – original draft. **Saulo de Toledo Pereira:** Data curation, Investigation, Visualization, Writing – original draft. **Maria Fernanda Setúbal Destro Rodrigues:** Formal analysis, Methodology, Writing – review & editing. **Arthur Cássio de Lima Luna:** Formal analysis, Methodology, Writing – review & editing. **Marcia Martins Marques:** Conceptualization, Methodology, Writing – review & editing. **Martha Simões Ribeiro:** Conceptualization, Formal analysis, Funding acquisition, Methodology, Project administration, Resources, Supervision, Writing – review & editing.

Declaration of Competing Interest

The authors declare that they have no known competing financial interests or personal relationships that could have appeared to influence the work reported in this paper.

Acknowledgments

We thank M.Sc. Antônio Santos Silva and Prof. Cristiane Miranda França for their technical assistance.

References

[1] The Skin Cancer Foundation, Skin cancer Facts & Statistics, Available at: https://www.skincancer.org/skin-cancer-information/skin-cancer-facts, 2021.
[2] B. Domingues, J.M. Lopes, P. Soares, H. Pópulo, Melanoma treatment in review, Immunotargets Ther. 7 (2018) 35–49.
[3] World Health Organization, Global Cancer Rates could Increase by 50% to 15 million by 2020, Available at, https://www.who.int/news/item/03-04-2003-global-cancer-rates-could-increase-by-50-to-15-million-by-2020. Accessed on February 2022.
[4] G.C. Leonardi, L. Falzone, R. Salemi, A. Zanghi, D.A. Spandidos, J.A. Mccubrey, et al., Cutaneous melanoma: from pathogenesis to therapy (review), Int. J. Oncol. 52 (2018) 1071–1080.
[5] S. Carr, C. Smith, J. Wernberg, Epidemiology and risk factors of melanoma, Surg. Clin. North Am. 100 (2020) 1–12.
[6] R.I. Hartman, J.Y. Lin, Cutaneous melanoma-a review in detection, staging, and management, Hematol. Oncol. Clin. North Am. 33 (2019) 25–38.
[7] S. Urbancek, P. Fedorcova, J. Tomkova, R. Sutka, Misdiagnosis of melanoma: a 7 year single-center analysis, J. Pigment Disord. 2 (2015) 1–4.
[8] H.Z. Gong, H.Y. Zheng, J. Li, Amelanotic melanoma, Melanoma Res. 29 (2019) 221–230.
[9] I. Kozar, C. Margue, S. Rothengatter, C. Haan, S. Kreis, Many ways to resistance: how melanoma cells evade targeted therapies, Biochim. Biophys. Acta Rev. Cancer. 1871 (2019) 313–322.
[10] T.J. Dougherty, S.L. Marcus, Photodynamic therapy, Eur. J. Cancer 28A (1992) 1734–1742.
[11] V. Heiskanen, M.R. Hamblin, Photobiomodulation: lasers vs. light emitting diodes? Photochem. Photobiol. Sci. 17 (2018) 1003–1017.
[12] F.F.C. Petz, J.V.C. Félix, H. Roehrs, F.S. Pott, J.G.D. Stocco, R.L. Marcos, et al., Effect of photobiomodulation on repairing pressure ulcers in adult and elderly patients: a systematic review, Photochem. Photobiol. 96 (2020) 191–199.
[13] F.C. da Silva, T. Silva, A.O. Gomes, P.R.C. Palácio, L. Andreo, M.L.L. Gonçalves, et al., Sensory and motor responses after photobiomodulation associated with physiotherapy in patients with incomplete spinal cord injury: clinical, randomized trial, Lasers Med. Sci. 35 (2020) 1751–1758.
[14] L.G. Langella, H.L. Casalechi, S.S. Tomazoni, D.S. Johnson, R. Albertini, R. C. Pallotta, et al., Photobiomodulation therapy (PBMT) on acute pain and inflammation in patients who underwent total hip arthroplasty-a randomized, triple-blind, placebo-controlled clinical trial, Lasers Med. Sci. 33 (2018) 1933–1940.
[15] R.J. Bensadoun, R.G. Nair, J. Robijns, Photobiomodulation for side effects of cancer therapy, Photobiomodul. Photomed. Laser Surg. 38 (2020) 323–325.
[16] R.J. Bensadoun, J.B. Epstein, R.G. Nair, A. Barasch, J.E. Raber-Durlacher, C. Migliorati, M.T. Genot-Klastersky, N. Treister, P. Arany, J. Lodewijckx, J. Robijns, World Association for Laser Therapy (WALT). Safety and efficacy of photobiomodulation therapy in oncology: a systematic review, Cancer Med. 9 (2020) 8279–8300.
[17] M.R. Hamblin, S.T. Nelson, J.R. Strahan, Photobiomodulation and Cancer: what is the truth? Photomed. Laser Surg. 36 (2018) 241–245.
[18] R. Zein, W. Selting, M.R. Hamblin, Review of light parameters and photobiomodulation efficacy: dive into complexity, J. Biomed. Opt. 23 (2018) 1–17.
[19] M.J. Mattes, T.M. Thomson, L.J. Old, K.O. Lloyd, A pigmentation-associated, differentiation antigen of human melanoma defined by a precipitating antibody in human serum, Int. J. Cancer 32 (1983) 717–721.
[20] L.S. Ferreira, I.M.A. Diniz, C.M.S. Maranduba, S.P.H. Miyagi, M.F.S.D. Rodrigues, C. Moura-Neto, et al., Short-term evaluation of photobiomodulation therapy on the proliferation and undifferentiated status of dental pulp stem cells, Lasers Med. Sci. 34 (2019) 659–666.
[21] L. Frigo, J.S.S. Luppi, G.M. Favero, D.A. Maria, S.C. Penna, J.M. Bjordal, et al., The effect of low-level laser irradiation (in-Ga-Al-AsP-660 nm) on melanoma in vitro and in vivo, BMC Cancer 9 (2009) 404.
[22] J.L. da Silva, A.F. Silva-de-Oliveira, R.A. Andraus, L.P. Maia, Effects of low level laser therapy in cancer cells—a systematic review of the literature, Lasers Med. Sci. 35 (2020) 523–529.
[23] M.H. Niemz, Laser-Tissue Interactions: Fundamentals and Applications, Third edition, Springer, 2007, p. 324.
[24] A. Oikawa, M. Nakayasu, Quantitative measurement of melanin as tyrosine equivalents and as weight of purified melanin, Yale J. Biol. Med. 46 (1973) 500–507.
[25] A.L. de Andrade, P.S. Bossini, N.A. Parizotto, Use of low level laser therapy to control neuropathic pain: a systematic review, J. Photochem. Photobiol. B Biol. 164 (2016) 36–42.
[26] S.L. Jacques, Optical properties of biological tissues: a review, Phys. Med. Biol. 58 (2013) 37–61.
[27] C. Contatori, C.R. Silva, M. Ribeiro, Effects of near-infrared low level laser irradiation on melanoma cells, in: R. Costa-Felix, J. Machado, A. Alvarenga (Eds.), XXVI Brazilian Congress on Biomedical Engineering. IFMBE Proceed 70/2, 2019, pp. 797–801.
[28] T. Osawa, M. Muramatsu, M. Watanabe, M. Shibuya, Hypoxia and low-nutrition double stress induces aggressiveness in a murine model of melanoma, Cancer Sci. 100 (2009) 844–851.
[29] C.E. Werneck, A.L.B. Pinheiro, M.T.T. Pacheco, C.P. Soares, J.L.F. de Castro, Laser light is capable of inducing proliferation of carcinoma cells in culture: a spectroscopic in vitro study, Photomed. Laser Surg. 23 (2005) 300–303.
[30] Y. Rai, R. Pathak, N. Kumari, D.K. Sah, S. Pandey, N. Kalra, et al., Mitochondrial biogenesis and metabolic hyperactivation limits the application of MTT assay in the estimation of radiation induced growth inhibition, Sci. Rep. 8 (2018) 1531.
[31] C.R. Silva, F.V. Cabral, C.F.M. de Camargo, S.C. Nunez, T.M. Yoshimura, A.C. D. Luna, et al., Exploring the effects of low-level laser therapy on fibroblasts and tumor cells following gamma radiation exposure, J. Biophotonics 9 (2016) 1157–1166.
[32] Y.A. Fouad, C. Aanei, Revisiting the hallmarks of cancer, Am. J. Cancer Res. 7 (2017) 1016–1036.
[33] I.J. Fidler, Biological behavior of malignant melanoma cells correlated to their survival in vivo, Cancer Res. 35 (1975) 218–224.
[34] T. Karu, Primary and secondary mechanisms of action of visible to near-IR radiation on cells, J. Photochem. Photobiol. B Biol. 49 (1999) 1–17.
[35] M.B. de Moura, G. Vincent, S.L. Fayewicz, N.W. Bateman, B.L. Hood, M. Sun, et al., Mitochondrial respiration–an important therapeutic target in melanoma, PLoS One 7 (2012), e40690.
[36] N.V. Andreeva, K.V. Zotov, Y.E. Yegorov, M.V. Kalashnikova, V.I. Yusupov, V. N. Bagratashvili, et al., The effect of infrared laser irradiation on the growth of human melanoma cells in culture, Biophys. 61 (2016) 979–984.
[37] G.D. Birkmayer, B.R. Balda, O. Braun-Falco, Differences in cytochrome oxidase and mitochondrial ATPase in melanotic and amelanotic melanoma, Arch. Klin. Exp. Dermatol. 239 (1970) 288–295.
[38] G. Ottaviani, V. Martinelli, K. Rupel, N. Caronni, A. Naseem, L. Zandonà, et al., Laser therapy inhibits tumor growth in mice by promoting immune surveillance and vessel normalization, Ebiomedicine. 11 (2016) 165–172.

[39] R.M. Slominski, T. Sarna, P.M. Płonka, C. Raman, A.A. Brożyna, A.T. Slominski, Melanoma, melanin, and melanogenesis: the Yin and Yang relationship, Front. Oncol. 12 (2022), 842496.
[40] A. Slominski, T.K. Kim, A.A. Brożyna, Z. Janjetovic, D.L. Brooks, L.P. Schwab, et al., The role of melanogenesis in regulation of melanoma behavior: melanogenesis leads to stimulation of HIF-1α expression and HIF-dependent attendant pathways, Arch. Biochem. Biophys. 563 (2014) 79–93.
[41] K.M. Vincent, L.M. Postovit, Investigating the utility of human melanoma cell lines as tumour models, Oncotarget 8 (2017) 10498–10509.